J. Physiol. (1983), **341**, 41–58
With 12 text-figures
Printed in Great Britain

THE SPATIAL DISTRIBUTION OF EXCITABILITY AND MEMBRANE CURRENT IN NORMAL AND DEMYELINATED MAMMALIAN NERVE FIBRES

BY H. BOSTOCK, T. A. SEARS AND R. M. SHERRATT

From the Sobell Department of Neurophysiology, Institute of Neurology, Queen Square, London WC1N 3BG

(*Received 13 January 1983*)

SUMMARY

1. Thresholds to electrical stimulation have been recorded, concurrently with the membrane currents of conducted impulses, at many positions along undissected single fibres in rat spinal roots.

2. In normal myelinated fibres, distinct threshold minima invariably coincided with sites of inward current generation, and were therefore identified as nodes of Ranvier. Between nodes, the thresholds rose by an order of magnitude.

3. At normal nodes, the charge thresholds were linearly related to stimulus duration, as predicted by computer simulations of a model myelinated fibre (Bostock, 1983). The strength–duration time constants averaged $64{\cdot}9 \pm 8{\cdot}3$ μsec (mean $\pm$ S.D.) at 37 °C, and had a Q_{10} of 1/1·39. They were relatively insensitive to changes in inter-electrode distance, or to partial anaesthetization with tetrodotoxin.

4. In fibres treated with diphtheria toxin 6–8 days previously, to induce paranodal or segmental demyelination, threshold minima were found both at nodes and in internodal regions generating inward membrane current. In these fibres strength–duration curves were of the same general form as at normal nodes, but with strength–duration time constants increased at widened nodes (up to 350 μsec) and at excitable internodes (600–725 μsec). Comparison with the computer model indicated that these changes were most likely due to exposure of axon membrane with a time constant much longer than that of the normal nodal membrane.

5. In none of the demyelinated fibres examined have we found any evidence of hyperexcitability.

INTRODUCTION

Symptoms in demyelinating disease have been classified as either negative (e.g. paralysis or sensory loss), due to impaired conduction, or positive (e.g. tic douloureux, paraesthesiae or paroxysmal attacks), attributed to ectopic impulse generation (Rasminsky, 1978). Studies of impulse conduction in undissected single demyelinated fibres have revealed the biophysical basis for the negative symptoms (Rasminsky & Sears, 1972; Bostock & Sears, 1978), and also how the conduction block may be reversed pharmacologically (Bostock, Sherratt & Sears, 1978), although a clinically useful drug has yet to be found. A comparable understanding of the positive

symptoms has not been achieved, although a variety of hyperexcitability phenomena have been described in experimental models, and the majority of positive symptoms respond to treatment with carbamazepine or diphenylhydantoin (Rasminsky, 1981). The experiments described here were undertaken to find out, as directly as possible, how electrical excitability is modified by demyelination, to shed light on the origin of the positive symptoms and to assist the search for a useful treatment for the negative symptoms in demyelinating disease (Sears, Bostock & Sherratt, 1978).

Excitability has been defined as the reciprocal of the current for excitation (Lussier & Rushton, 1952) and we have measured excitability using a modification of Lussier & Rushton's (1952) collision technique for determining thresholds of single undissected nerve fibres. Their method, originally applied to desheathed frog nerves to determine that a single fibre is excitable only at the nodes, was later used by Coppin & Jack (1971) to measure internodal lengths in desheathed cat semitendinosus nerve. We have now combined this method with the technique of membrane current recording and mapping described previously (Bostock & Sears, 1978), to allow effectively simultaneous measurement of thresholds and currents through the same tripolar electrode assembly.

We describe here the spatial distributions of electrical excitability found by this dual technique in normal fibres and those demyelinated with diphtheria toxin, and also their strength–duration curves. We have found that the strength–duration curves follow a simple, non-exponential relationship, which is changed in a characteristic way by demyelination. To understand the biophysical basis for this, the factors affecting strength–duration curves have been explored with a computer model (Bostock, 1983). The results confirm previous evidence that the axon membrane exposed by demyelination has a much higher time constant than normal nodal membrane (Chiu & Ritchie, 1981; Brismar, 1981; Lafontaine, Rasminsky, Saida & Sumner, 1982). We have not found any evidence for hyperexcitability in these demyelinated axons.

A brief preliminary report on the method has been published (Bostock, Forster, Sears & Sherratt, 1981).

METHODS

All the experiments were conducted on adult male Wistar rats weighing 180–250 g. The methods for inducing demyelination and preparing the animals for recording were as described by Bostock & Sears (1978). Briefly, demyelination was achieved by intrathecal injection of a few microlitres of diphtheria toxin solution, between petroleum jelly seals, under sodium pentobarbitone anaesthesia. The terminal experiments were carried out under anaesthesia with urethane (1·25 g/kg I.P., supplemented as required) on operated animals 6–8 days after toxin injection, or on un-operated controls. The spinal roots of the cauda equina were exposed by laminectomy and lifted onto oxygenated liquid paraffin (Evans, B.P.C.) warmed by an infra red heater; temperature control was the same as described by Bostock, Sears & Sherratt (1981).

Recording and stimulation arrangements

The two operations of threshold determination and membrane current recording were performed during alternate cycles of the controlling pulse generator (Digitimer), designated for convenience as cycle 'A' and cycle 'B'. In cycle 'A' threshold tracking took place and in cycle 'B' membrane current determination and recording of longitudinal current calibration signals took place. Three sets of electrodes were used (Fig. 1*A*, *B*), a caudal pair (the trigger electrodes) for recording spikes propagating rostrally in ventral root axons stimulated (S_1) in the tail, a rostral electrode for

injecting a longitudinal current calibration pulse, and a movable tripolar electrode in between. The tripolar electrode was held in a micromanipulator (Narashige, Japan) and driven rostrally or caudally by a stepping motor in approximately 5 μm steps. The direction of travel and the number of steps were relayed to a PDP 11/34 (Digital Equipment Corporation) computer, which was also used for tracking the thresholds and storing membrane current wave forms. Maximum traverse was about 6·5 mm.

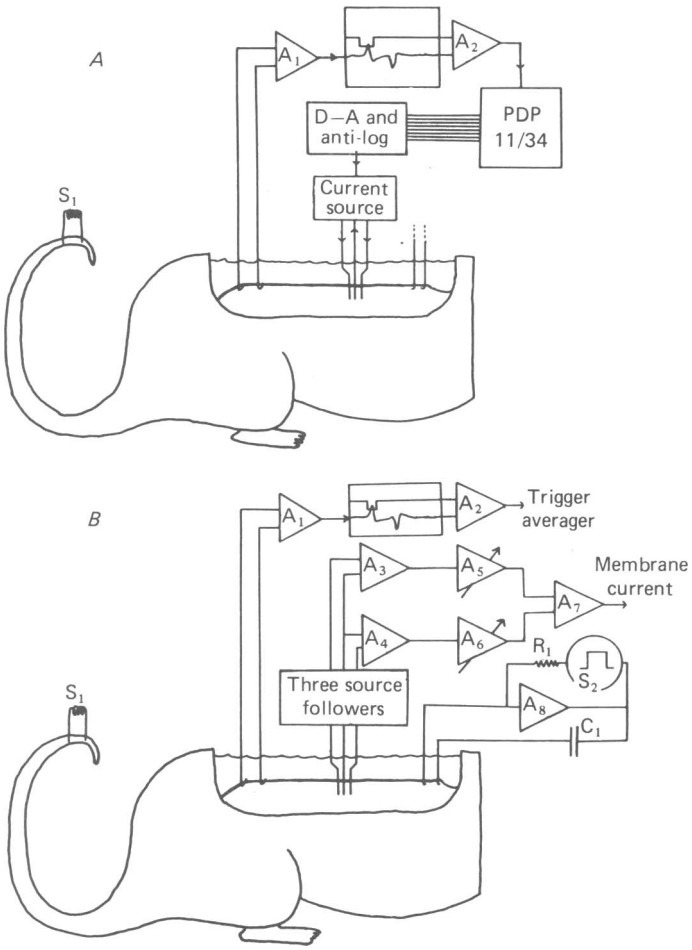

Fig. 1. Schematic diagrams of recording and stimulation arrangements, showing (*A*) configuration for finding thresholds (cycle 'A'), and (*B*) for recording membrane currents (cycle 'B'), as described in text.

Cycle 'A': threshold determination

In cycle 'A', the threshold for excitation was determined by the occurrence or non-occurrence of a collision between a securely repeating impulse, propagated rostrally from the tail and one propagated caudally from the tripolar electrode in the middle of the root, the point of detection being the trigger electrodes connected to the amplifier A_1. The impulse was detected using the voltage-latency window, also used for spike-triggered averaging (Bostock & Sears, 1978). When the control impulse was occurring reliably, the second, test stimulus of adjustable amplitude was delivered to the root by the tripolar electrode (middle, cathode; outer, anodes). The stimulus on

the root was delivered by a specially designed constant-current stimulator, described separately, the amplitude being constantly varied to straddle the threshold. During cycle 'B', when no stimulus was delivered to the root, the tail stimulus was delivered as normal, and a buzzer warned if the impulse failed to reach the trigger electrodes.

The amplitude of the test stimulus was under the control of the PDP 11/34 computer, and adjusted according to whether or not a collision had occurred. An eight-bit word from the computer was converted to a voltage, usually from 0·1 to 10 V in 2 % steps, by an analogue-to-digital convertor (D–A) and two-decade anti-logarithmic amplifier (see Fig. 1*A*). This control voltage, which was monitored by the computer, was converted to current in the range 1–100 μA by the stimulator (see below). A threshold estimate was registered by the computer when successive test stimuli were alternately ineffective and effective in producing a collision. Two pre-set stimulus durations were selected by the computer on alternate 'A' cycles, and threshold tracking carried out independently for each of the durations.

Cycle 'B': membrane current recording

The tripolar electrode was also connected as two differential recording pairs using amplifiers A_3 and A_4 (Fig. 1*B*), the centre electrode being common to both, and with each pair registering external longitudinal current. Membrane current is derived by subtracting adjacent longitudinal currents (Huxley & Stampfli, 1949), but before this can be done, the longitudinal current signals require scaling to allow for variations in root resistance. In contrast to previous experiments (Bostock & Sears, 1978), the scaling and subtraction were achieved by analogue circuits acting on the 'raw' signals. The current calibrations from each half of the tripole were compared separately with a reference, and the gain of each pre-amplifier (A_5 and A_6) adjusted accordingly. After a final differential stage (A_7), the membrane current signal was available for inspection and spike-triggered averaging (Datalabs DL102A). The averages, usually of thirty-two or sixty-four sweeps, were transferred to the PDP 11/34 computer for storage on disk and plotting. The analogue circuits invariably produced excellent gain adjustments, and subtraction led to the disappearance of the longitudinal current calibrations. One disadvantage of this arrangement was that information about the inter-electrode resistance of the spinal root was lost. To retain this information the calibrations were sampled prior to the variable gain and final differential stages, and converted by the computer to resistance. Changes in resistance usually indicated the accumulation of drops of fluid on the electrodes with consequent shunting of current.

Combined three-channel source follower and tripolar constant current stimulator

At first we attempted to alternate between stimulation and recording cycles by means of reed relays or analogue switches, but the switching transient induced in either case caused massive stimulation of spinal root axons. To overcome this we combined both functions in one circuit. For each of the three channels, the input was led via a 1·0 μF blocking capacitor to the gate of a 2N3819 field effect transistor (f.e.t.), which was connected in the cascode configuration to another 2N3819 to minimize input capacitance. The output from the source of the first f.e.t. provided the input for the longitudinal current differential amplifier (A_3 or A_4 in Fig. 1*B*: Devices 3160), and also fed a dual operational amplifier (J-FET '353'). The first half of the '353' was connected as a follower which drove the second half connected as a subtractor, and after subtraction of a stimulus control voltage (V_s) the signal was fed back to the gate of the input f.e.t. via a 10,000 pF capacitor and 100 kΩ resistor. The gain in the closed loop was adjusted accurately to 1·0, so that feed-back did not alter the gain. (It did, however, increase the noise.) The effect of a change in V_s was to drive a current of V_s/100 kΩ (or 10 μA/V) through the input. The a.c. coupling was found necessary to ensure d.c. stability. The time constant of 1 msec (= 10,000 pF × 100 kΩ) was chosen to be short relative to the interstimulus interval (130–330 msec) so that a negligible amount of current was still flowing at the time the next recording was made and as long as possible relative to the stimulus durations (usually 10 and 100 μsec). The three stimulus control voltages (V_s) were derived from the output of the anti-logarithmic circuit, which was connected by a DG200 analogue switch for the duration of the stimulus, and accurately multiplied by the factors $-1/2$, 1, $-1/2$ to provide a balanced tripolar stimulus.

Solutions

The Ringer solution contained: 131 mM-sodium, 5 mM-potassium, 2 mM-calcium, 111 mM-chloride and 29 mM-lactate, available as compound sodium lactate injection B.P. (Travenol Laboratories). It was adjusted to pH 7·4 and oxygenated before use. Tetrodotoxin (TTX; Sigma Chemicals) was dissolved in this solution. To treat a particular node that was being recorded, the tripolar electrode was withdrawn, and a droplet of the solution applied to the root for about 30 sec before being sucked off. Correct replacement of the electrode was confirmed by checking that inward membrane current was at a maximum.

RESULTS

Normal fibres

Spatial distribution of threshold and current

To map the electrical excitability of single fibres in terms of threshold and current, the tripole was moved continuously along the root at about 5 μm/sec by a stepping motor and micromanipulator. Membrane current wave forms were averaged ($n = 32$) and saved with the thresholds averaged over the same time period. Normally the tripole moved about 50 μm between averages, and about 50 μm during each average. Fig. 2*A* shows the spatial distribution of threshold measured in this way for a normal ventral root fibre at 37 °C, plotted on a logarithmic scale to encompass the 50-fold range of thresholds. The two curves were generated by stimuli of 10 and 100 μsec duration, to enable the strength–duration time constants to be estimated (see below). In Fig. 2*B* the membrane currents, at corresponding positions, are plotted as a contour map, as done by Bostock & Sears (1978). The concentric continuous rings correspond to peaks of inward membrane current, and therefore reveal the excitation of nodes, while the dashed lines indicate outward membrane current. This fibre therefore had a mean internodal length of about 1·25 mm, and a mean internodal conduction time of 19 μsec.

Comparison of Figs. 2*A* and *B* shows that threshold minima were found as expected at the nodes, and this has invariably been the case for normal fibres. Away from the nodes the thresholds rise along a characteristic curve, until they reach the curve of the next node, or the limiting current of the stimulator, or an unstable plateau, as in this case (see Discussion). The variation in threshold with distance could be recorded in more detail if membrane current averaging was dispensed with and thresholds averaged over shorter distances (see Fig. 6 below). The shape of these curves can be understood from the arguments of Lussier & Rushton (1952). The tripole sets up a triangular potential gradient along the root and if current enters and leaves the fibre only at the nodes, the excitability of the fibre (1/threshold) should have the same triangular profile. In practice this was an approximation (see Fig. 3): the triangular profiles were somewhat rounded, since myelin is not a perfect insulator, and the bases of the triangles were considerably wider than the tripole, probably because of the way the pia-arachnoid sheath affected the path of current flow.

Strength–duration curves

The variation of threshold with stimulus duration was examined in ten normal fibres at 37 °C. The tripole was first centred on a node, so that inward membrane

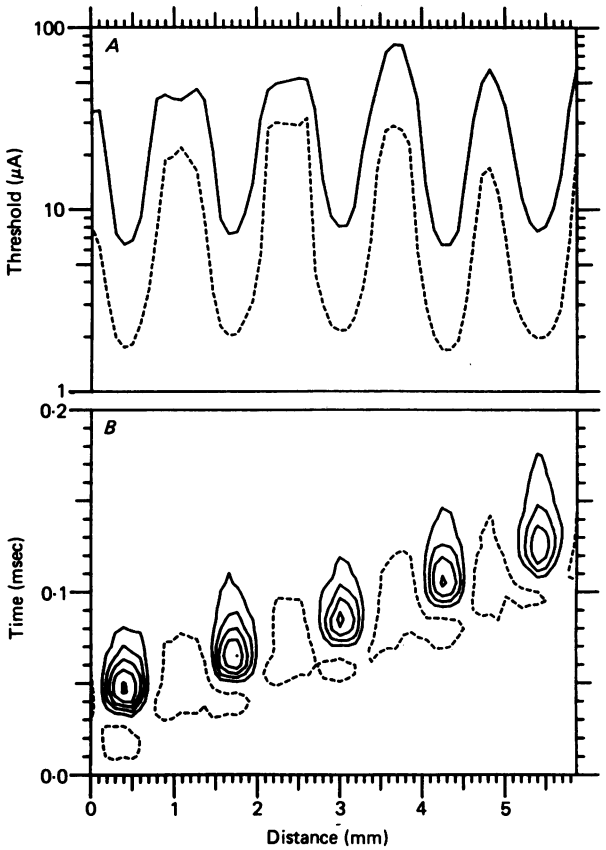

Fig. 2. Thresholds (*A*) and membrane currents (*B*) recorded together at many positions along an undissected single fibre in a normal ventral root at 37 °C. *A*, continuous line: thresholds to 10 μsec stimuli; dashed line: thresholds to 100 μsec stimuli. Note logarithmic scale. *B*, contour lines join points of equal membrane current density. Continuous lines: net inward current; dashed lines: net outward current. Contour interval: 1·5 nA.

current was maximal and threshold at a minimum. Thresholds were then determined with stimuli of alternating durations, one of which was fixed at 100 μsec and the other stepped from 10 to 200 μsec (see Fig. 4). Average threshold estimates for each stimulus duration were plotted every 2 sec and with a total stimulation rate of 6·5/sec (half of which were controls to ensure that triggering was stable) threshold estimates stabilized within a few seconds.

The data from Fig. 4 are plotted as a strength–duration curve in Fig. 5*A*. To test the shape of the curve, the two extreme points were used to predict the intervening ones according to two different equations. The continuous line is Weiss' (1901) empirical equation:

$$Q = Irh(t+\tau_{sd}), \tag{1}$$

where Q is the stimulus charge ($\int I.\,dt$), Irh is the rheobasic current, and τ_{sd} the strength–duration time constant. The dashed line is the 'classical' strength–duration equation of Lapicque (1907), i.e. $I = Irh/(1-\exp(-t/\tau_{sd}))$, modified slightly to allow

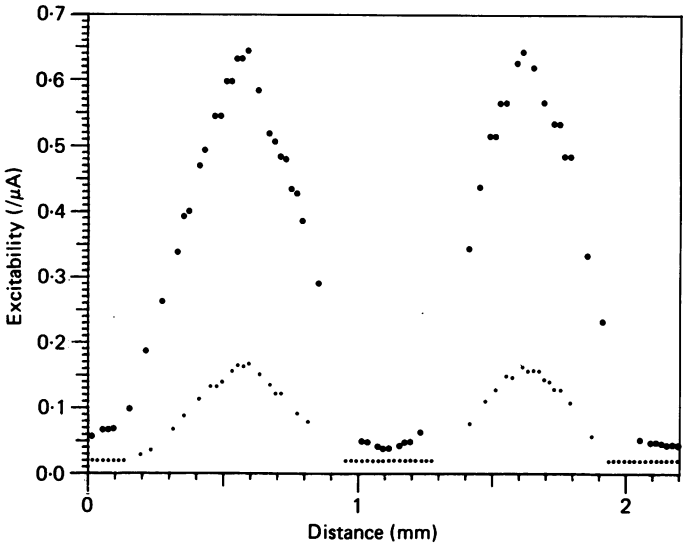

Fig.3. Excitability (1/threshold) of a single axon as a function of distance along a spinal root, for stimuli of 10 μsec (small filled circles) and 100 μsec (large filled circles) duration. Electrode separation: 350+350 μm.

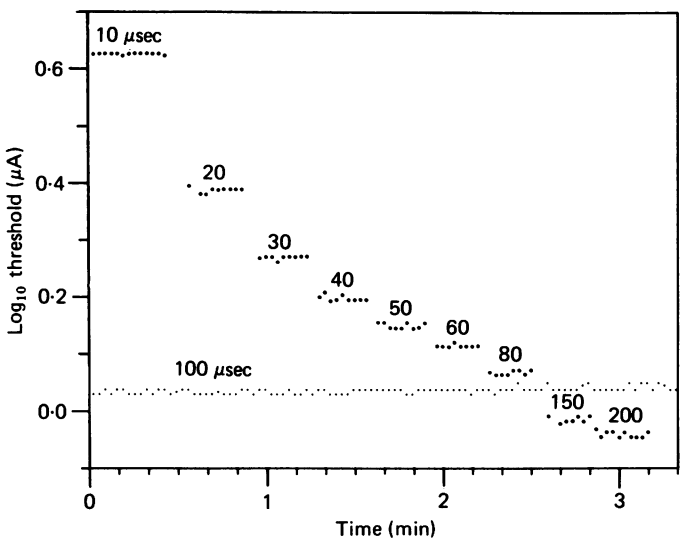

Fig. 4. Sequence of threshold estimates for stimuli of different durations recorded from a normal node (see text).

for the time constant (RC = 1 msec) of the stimulator (cf. Hill, 1935):

$$I = \frac{Irh(1-\tau_{sd}/RC)}{(e^{-t/RC}-e^{-t/\tau_{sd}})}. \quad (2)$$

It is evident that Weiss' equation provides a much better fit, and this was invariably the case. The modification of Lapicque's equation proposed by Hill (1936) did not improve the fit. Similar results have been obtained for a model myelinated fibre

(Bostock, 1983: see Fig. 3). In Fig. 5*B* the charge threshold is plotted against stimulus duration, and the straight line given by eqn. (1) projected to negative stimulus durations as done by Tasaki (1939), since it cuts the zero charge axis at $t = -\tau_{sd}$ and gives a graphical estimate of the strength–duration time constant (54·6 μsec). The rheobase is given by the slope of the line, dQ/dt (0·65 μA).

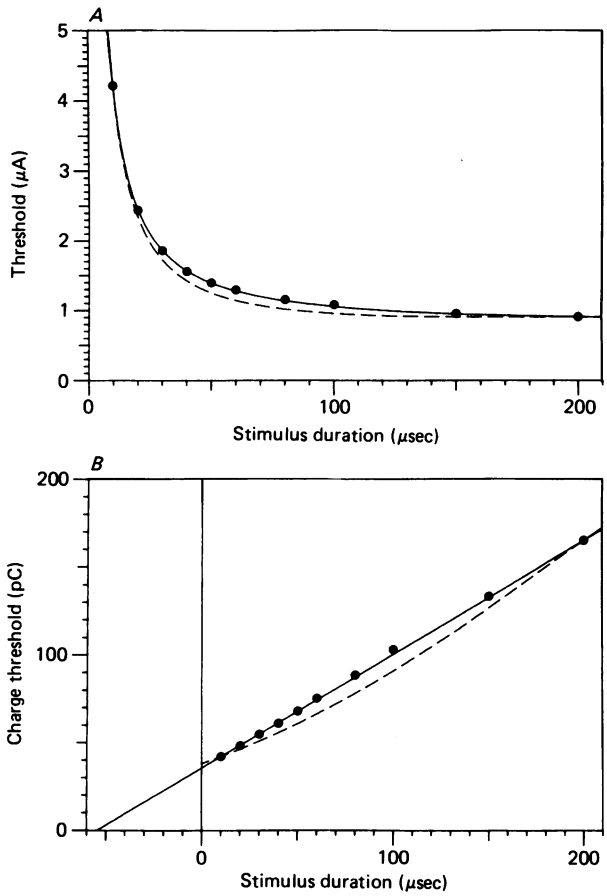

Fig. 5. Threshold data from Fig. 4 plotted (*A*) as a conventional strength–duration curve, and (*B*) as charge thresholds. Filled circles represent experimental data. Curves obtained by using extreme data points to fit Lapicque's formula (eqn. (2), dashed line) and Weiss' formula (eqn. (1), continuous line). Extrapolation of the continuous line to the zero charge axis in (*B*) gives an estimate of the strength–duration time constant.

Accepting that our data were satisfactorily described by eqn. (1), we estimated *Irh* and τ_{sd} by linear regression of Q on t. For ten normal fibres at 37 °C, τ_{sd} lay between 54 and 80 μsec (mean 64·9, S.D.: 8·3 μsec), while *Irh* ranged from 0·49 to 0·91 μA (mean 0·69, S.D.: 0·12 μA). Deviations of the fitted equations from the threshold estimates were not large, considering the precision of the measurements; the r.m.s. percentage error was 2·5% over-all, while the stimuli were altered in 2% steps. The range of rheobase values was fortuitously small, reflecting the selection of large motor fibres

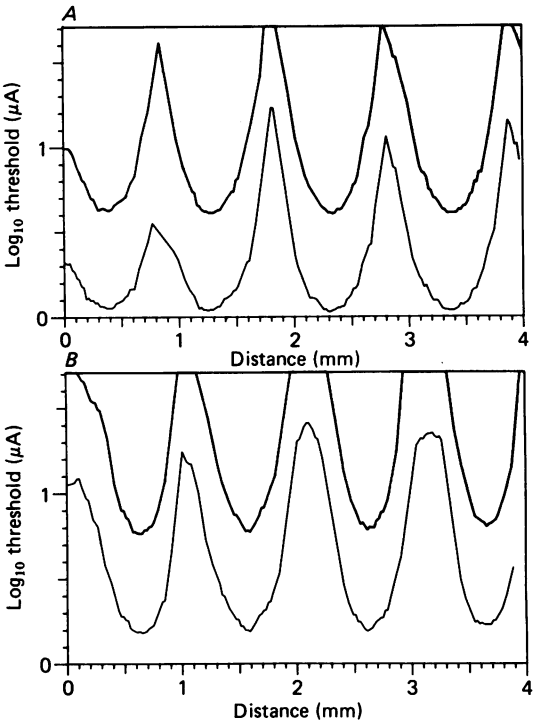

Fig. 6. Spatial distributions of threshold in one fibre recorded with different electrode separations. Stimulus durations: 10 μsec (bold trace) and 100 μsec (fainter trace). Tripolar electrodes were separated by (*A*) 750+750 μm, (*B*) 350+350 μm. (The zeros on the abscissae are arbitrary and do not quite correspond.)

in ventral roots of similar diameter. Taking into account the measured inter-electrode resistances (18–31 kΩ), the rheobasic currents corresponded to voltage drops across the electrodes of 7·5 $\pm$ 1·3 mV. For a fibre with an internodal axial resistance of 20 MΩ, this would correspond to an 'effective stimulating current' (Fitzhugh, 1962) of 0·75 nA.

Cruder estimates of the strength–duration time constant could be made from the thresholds at just two stimulus durations, such as the 10 and 100 μsec threshold estimates in Fig. 2*A*. These two-point estimates proved to be consistently lower (by about 16%) than the 10 point least-squares estimates, because eqn. (1) consistently over-estimated the thresholds for brief stimuli, as it did for the model nerve (Bostock, 1983). Thus for the ten normal fibres already considered, the two-point estimates for τ_{sd} averaged 54·3 $\pm$ 7·3 μsec (mean $\pm$ S.D.), while for thirty-two other normal nodes, whose full strength–duration curves were not measured, τ_{sd} averaged 55·8 $\pm$ 8·6 μsec (mean $\pm$ S.D.).

Factors affecting normal thresholds

Electrode separation. In some preparations, strength–duration time constants are highly dependent on stimulus geometry (Davis, 1923; Noble & Stein, 1966). To test this possibility in our preparation, we scanned the same four nodes in one fibre with

stimuli of 10 and 100 μsec, using first a tripole with electrodes 750+750 μm apart (Fig. 6*A*) and then a tripole with electrodes 350+350 μm apart (Fig. 6*B*). Spatial resolution was improved somewhat with the more closely spaced electrodes, and estimates for *Irh* increased (from 0·72, 0·70, 0·69 and 0·71 μA to 0·95, 0·98, 0·95 and 1·07 μA), but the estimates for τ_{sd} changed only slightly (from 48, 48, 48 and 47 μsec to 52, 52, 54 and 52 μsec).

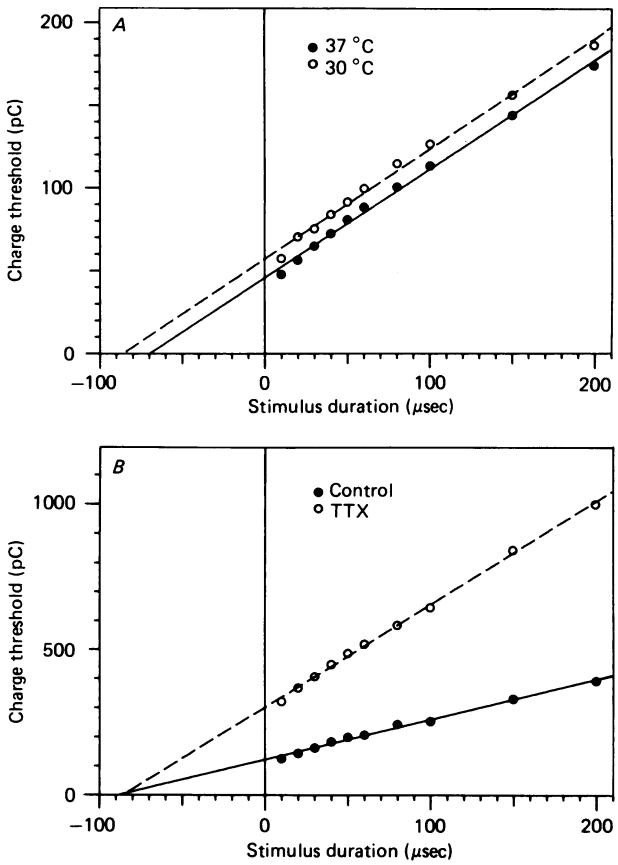

Fig. 7. Typical effects of temperature (*A*) and TTX (*B*) on charge threshold–duration relationship. Temperature primarily affects the strength–duration time constant (intercept on zero charge axis), while TTX primarily affects rheobasic current (slope).

Temperature. Strength–duration curves for six nodes were recorded at both 30 and 37 °C (e.g. Fig. 7*A*). Strength–duration time constants were increased by a factor of 1·26±0·05 (mean ±S.E. of the mean) with a fall of 7 °C, corresponding to a Q_{10} of 1/1·39. Rheobases fell by a factor of 0·86±0·05 (mean ±S.E. of the mean). For one normal node the thresholds to 10 and 200 μsec stimuli were estimated repeatedly, while the temperature was changed in steps, and τ_{sd} estimated at each temperature. The temperature variation of τ_{sd} was well fitted by an exponential (see Fig. 8), corresponding to a Q_{10} of 1/1·42, which is in good agreement with the previous estimate. These temperature variations of the strength–duration relationship lie

between the two cases simulated (Bostock, 1983), but closer to the first case, in which only rate constants and maximum permeabilities were assumed to change with temperature. When the model was extrapolated to 37 °C with these assumptions, and tripolar stimulation used, the strength–duration time constant became 66 μsec, close to the experimental average of 65 μsec reported here for rat nodes at 37 °C.

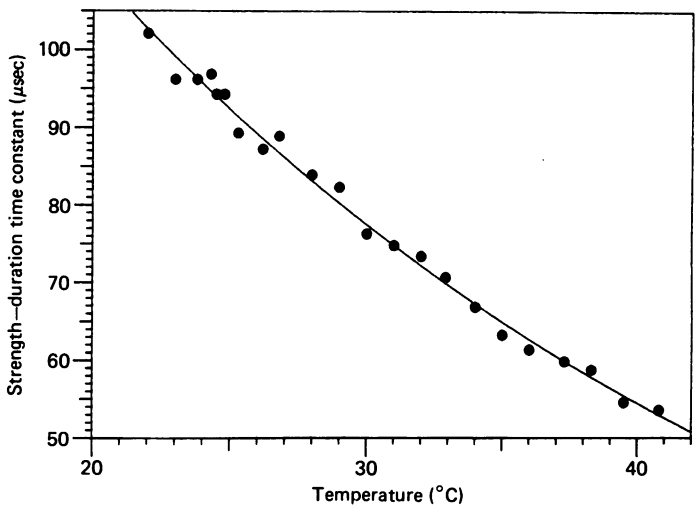

Fig. 8. Variation of the strength–duration time constant with temperature for a normal node. Thresholds were repeatedly estimated using stimuli of 10 μsec and 200 μsec duration. The curve, obtained by regression of log time constant on temperature, corresponds to a Q_{10} of 1/1·42.

Sodium permeability. Strength–duration curves were recorded for one normal node, before and after applying a drop of 50 nM-TTX (Fig. 7*B*). The rheobasic current was increased by 155 %, while the strength–duration time constant was reduced by only 3 %. Similar selective action of TTX on the rheobase was observed at two other nodes. This response to a reduction in maximum sodium permeability differed from that of the model nerve at 20 °C (Table 1 in Bostock, 1983), which predicted a significant increase in the strength–duration time constant with block of sodium channels. Re-running the model at 37 °C, however, predicted for a block of 75 % of sodium channels an increase in *Irh* of 31 % and a negligible change in τ_{sd} (−1 %).

Fibres chronically demyelinated with diphtheria toxin

Conduction in rat spinal root fibres demyelinated with diphtheria toxin has previously been described in terms of membrane current recordings (Rasminksy & Sears, 1972; Bostock & Sears, 1978). A common abnormality is delayed saltatory conduction, attributed to paranodal demyelination (Rasminsky & Sears, 1972), but in some fibres, with more extensive loss of myelin, conduction becomes continuous, with electrical excitability distributed along one or more internodes (Bostock & Sears, 1978). In this study the demyelinated fibres were recorded at 30 °C, to increase the safety factor for conduction (Rasminsky, 1973).

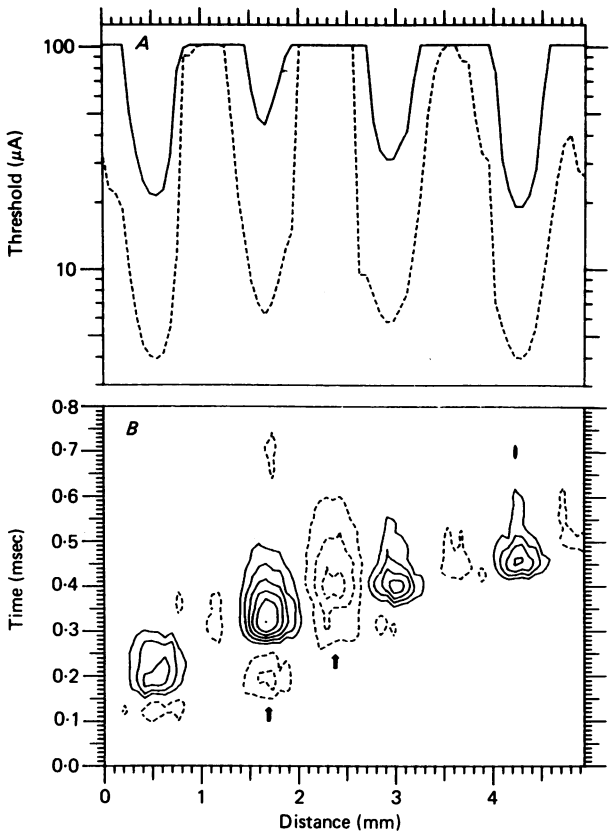

Fig. 9. Thresholds (*A*) and membrane currents (*B*) recorded from undissected axon 8 days after treatment with diphtheria toxin to cause paranodal demyelination. Arrows indicate presumed sites of demyelination (see text). *A*, thresholds plotted on log scale for 10 μsec (continuous line) and 100 μsec (dashed line) stimuli. *B*, contour map of membrane currents plotted as in Fig. 2*B*.

Paranodal demyelination

Fig. 9 shows membrane current contours and thresholds at 30 °C for a fibre recorded 8 days after intrathecal injection of diphtheria toxin. Conduction was slow, particularly from the first node to the second (110 μsec) and the distribution of outward membrane currents suggests that myelin had been lost mainly from the paranode of the second node, and from the internode following (i.e. the arrowed sites). The thresholds to stimuli of 10 and 100 μsec again had minima at the nodes, and the threshold currents for the longer stimulus showed no clear correlation with the extent of demyelination (whether inferred from internodal conduction times or from the amount of outward membrane current). The ratio between the two thresholds was, however, unusually high at the second node, corresponding to a strength–duration time constant of 271 μsec, compared with 105 μsec at nodes 1 and 3, and a nearly normal value of 80 μsec at node 4. (This node also required the least outward current to be excited by the conducted impulse.)

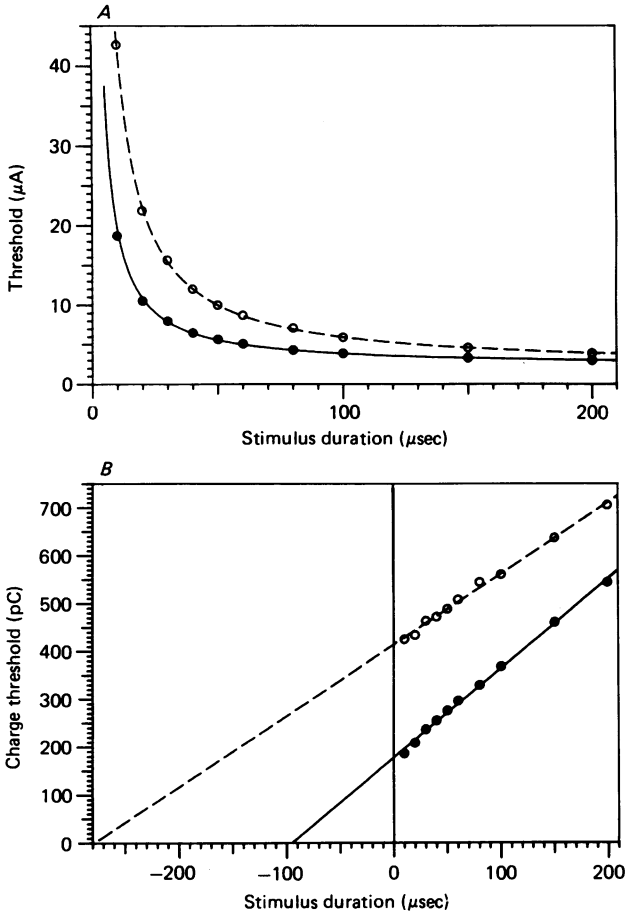

Fig. 10. Strength–duration curves plotted in terms of current (*A*) and charge (*B*) for the arrowed node 2 (open circles) and the relatively normal node 4 (filled circles) of Fig. 9. The intercepts of the fitted lines in (*B*) indicate the much longer strength–duration time constant at the widened node.

To confirm these time-constant estimates, we then recorded strength–duration curves at nodes 2 and 4, and these are plotted in Fig. 10. The points were again well fitted by Weiss' formula, and yielded estimates for the strength–duration time constant of 279 ± 10 μsec at node 2, and 95 ± 6 μsec at node 4, in reasonable agreement with the two-point estimates. Interestingly, the rheobase was lower at node 2 (1·5 as against 1·9 μA at node 4), although not abnormally low in relation to normal nodes. Strength–duration curves recorded at five other nodes, presumed from their membrane currents to be widened following exposure to diphtheria toxin, have given estimates for τ_{sd} in the range 240–350 μsec. These figures compare with the range of 75–93 μsec recorded at six normal nodes at 30 °C. This effect is probably not peculiar to demyelination caused by diphtheria toxin; long strength–duration time constants have also been indicated by the ratios between thresholds to long and short stimuli recorded from fibres demyelinated with lysolecithin, although full strength–duration

curves have not been recorded (H. Bostock, R. M. Sherratt & T. A. Sears, unpublished observations). Rheobases have been altered in a less consistent fashion, but in no case has an abnormally low rheobase been recorded.

Segmental demyelination with continuous conduction

Fig. 11 shows membrane current contours and thresholds at 30 °C for another fibre, recorded 8 days after diphtheria toxin injection. The recording covers a stretch of

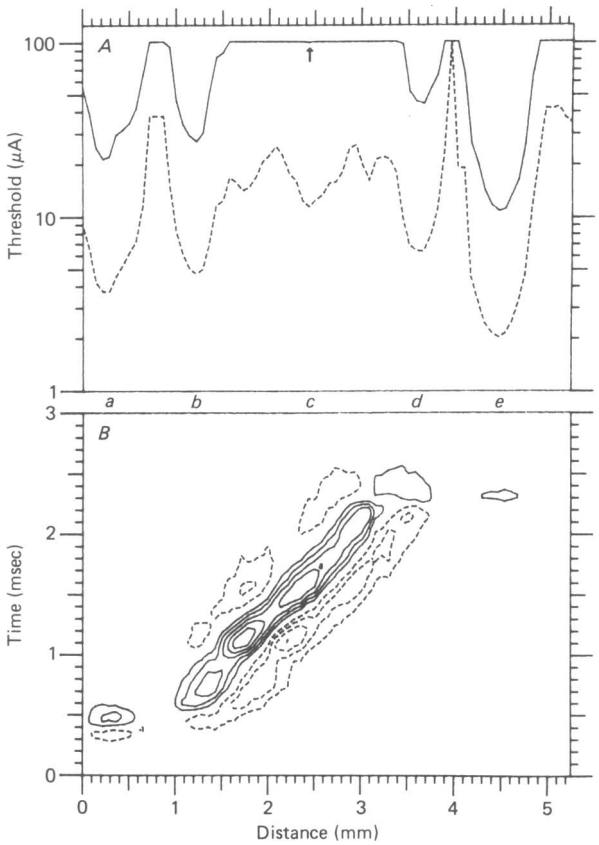

Fig. 11. Thresholds (*A*) and membrane current contour map (*B*) recorded from undissected axon 8 days after treatment with diphtheria toxin,causing segmental demyelination with continuous conduction. Letters *a* to *e* indicate positions along fibres referred to in text. Stimulus durations in (*A*): 10 μsec (continuous line) and 100 μsec (dashed line).

slow conduction (1·25 m/sec) which was continuous within the limits of resolution of the tripole. The thresholds to stimuli of 10 and 100 μsec had minima of the normal shape at the nodes at either end (*a*, *e*), and at the two edges of the demyelinated stretch (*b*, *d*), but the estimated strength–duration time constants were long, especially at site *d* (258 μsec), as at the widened nodes in Fig. 9. The thresholds varied irregularly in the demyelinated stretch, and were high; indeed for the 10 μsec stimulus they were off scale except at *c* (see arrow). This one point corresponded to a very long strength–duration time constant (718 μsec), but relatively normal rheobase (1·37 μA).

To confirm this we scanned the root again with stimulus durations of 30 and 300 μsec, and obtained estimates of 609 μsec for τ_{sd} and 1·46 μA for *Irh* at *c*. The threshold ratio (and hence estimate) was much the same throughout the demyelinated stretch.

To check the validity of these two-point threshold estimates, we then recorded strength–duration curves, with stimulus durations extended to 500 μsec, at *c* and *e*. The data were again fitted well by Weiss' formula (see Fig. 12; a log–log plot was used because of the wide stimulus range), and gave strength–duration time-constant

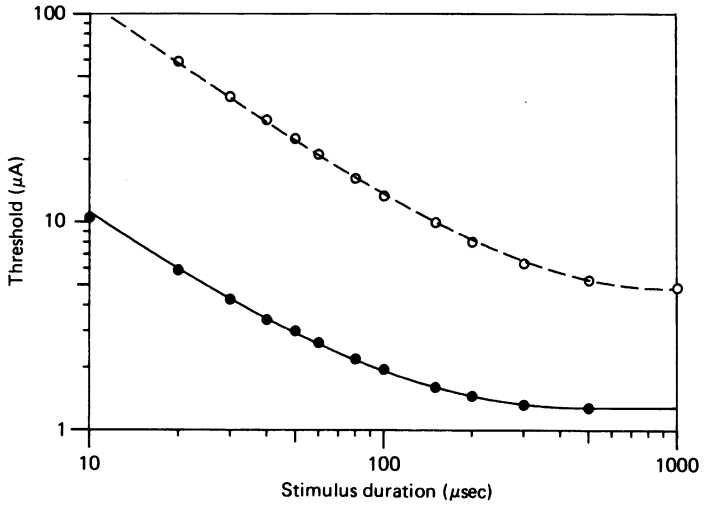

Fig. 12. Strength–duration curves recorded at two sites in a fibre demyelinated with diphtheria toxin (see Fig. 11), plotted on double logarithmic co-ordinates. Open circles correspond to demyelinated site *c*, fitted with curve for τ_{sd} = 606 μsec; *Irh* = 1·8 μA. Filled circles recorded at node *e* in Fig. 11, fitted with curve for τ_{sd} = 127 μsec; *Irh* = 0·8 μA.

estimates of 606 and 127 μsec at *c* and *e* respectively, and rheobases of 1·8 and 0·8 μA. The strength–duration curve was also recorded for an excitable internode in a 6-day diphtheria toxin lesion, and the least-squares fit to the charge thresholds this time gave τ_{sd} as 725 μsec and *Irh* as 3·4 μA. The strength–duration curves in segmental demyelination may not be strictly comparable with those in normal and paranodally demyelinated fibres, because of the different paths available for current flow, but it is reasonable to conclude that they are distinguished by even longer strength–duration time constants.

DISCUSSION

In this paper we have, firstly, shown how the distribution of threshold along single mammalian nerve fibres can be mapped *in vivo*, and compared with the membrane currents occurring during impulses conducted in the same fibres. Secondly, we have shown how thresholds are altered in demyelination. The use of a tripolar electrode for focal stimulation, and a collision technique for isolating the threshold of a single un-dissected fibre were described by Lussier & Rushton (1952), who used the method

to show that desheathed frog fibres are excitable only at nodes. They used a fixed, strong stimulus, and simply noted that short, excitable lengths of nerve alternated with longer, inexcitable lengths. Coppin & Jack (1971) applied Lussier & Rushton's technique to a mammalian preparation, desheathed cat semitendinosus nerve, but only published data on the derived internodal lengths. We have used a more convenient mammalian preparation, the spinal roots of the rat cauda equina, which have so little connective tissue that desheathing is not required. We have also extended the threshold-mapping technique in three important ways: (1) by automatic tracking of thresholds over a 100-fold range, we have been able to produce accurately reproducible plots of threshold against distance; (2) by the use of a combined tripolar pre-amplifier/stimulator, we have been able to alternate threshold estimations rapidly with membrane current recordings at the same site and (3) by alternating stimulus durations, we have been able to estimate strength–duration time constant and rheobase at each site.

The shape of the threshold *vs.* distance plots for normal fibres was much as expected from the arguments of Lussier & Rushton (1952). To a first approximation a node was only excited when straddled by the tripole, when the excitability (1/threshold) was roughly proportional to the difference in extracellular potential between that node and adjacent nodes (Fig. 3). We have routinely plotted thresholds on a logarithmic scale (e.g. Figs. 2*A*, and 6), partly to encompass the wide range of thresholds encountered, but also because threshold or excitability ratios are usually of more interest than absolute differences. We have not attempted to interpret the high 'thresholds' recorded when the tripole was not straddling a node, which were usually 10 or more times higher than the nodal thresholds, and were also distinguished by their instability, and by their failure to fall on a sensible strength–duration curve. We found that the 'thresholds' recorded in mid-internode would increase when the stimulus duration was increased beyond a certain limit, or even that two 'thresholds' could be recorded for the same stimulus duration. On the basis of these observations we adopted two criteria for accepting that a threshold estimate reflected the excitability of the area of axon opposite the centre of the tripole: (1) the threshold should be at a minimum of the threshold *vs.* distance plot and (2) that a 'sensible' strength–duration curve should be recordable, i.e. that threshold current should decrease monotonically with increasing stimulus duration over a wide stimulus range.

In fibres demyelinated with diphtheria toxin, 'sensible' strength–duration curves were recordable both at widened nodes and in internodes which sustained continuous conduction, but the time constants for excitation were much increased. To quantify these changes we used Weiss' (1901) formula (eqn. 1), which fitted the data from both normal and demyelinated fibres much better than the 'classical' strength–duration equations of Lapicque (1907) or Hill (1936), in agreement with computer simulations (Bostock, 1983). Thus using a least-squares fit to eqn. (1), the normal strength–duration time constant at 30 °C of 84 μsec was altered by paranodal demyelination to 279 μsec or more (Fig. 10). Was this change simply due to the extra area of membrane being depolarized, or did it imply a change in membrane properties? The simulation study (Bostock, 1983) showed that a simple increase in nodal area (without a change in membrane time constant) should *decrease* the strength–duration time constant, whether the additional membrane contained

sodium channels or not. For demyelination to increase strength–duration time constants, the additional axon membrane exposed should have a membrane time constant much higher than that of the original node. (The alternative of a slowing of sodium activation kinetics seems unlikely.) Thus we conclude that the increases in strength–duration time constant occurring with demyelination are due to increases in average membrane time constant, although a one-to-one relationship is not expected. Comparable increases in membrane time constant have recently been recorded in isolated rat fibres previously treated with diphtheria toxin: Brismar (1981) found that the normal time constant of 50 ± 12 μsec (mean ±S.D.) at 25 °C increased with paranodal demyelination to 150–550 μsec and estimated a time constant for the axolemma previously covered with myelin of about 1500 μsec.

In one respect our results have been negative. We have found no evidence from our threshold measurements for any hyperexcitability due to demyelination. Thresholds to standard stimuli have always been higher at sites of demyelination and even though the calculated rheobases have not been elevated in the same way, because of the change in shape of the strength–duration curve, they have never been abnormally low. Hyperexcitability, whether expressed as spontaneous activity, or activity evoked by normally non-excitatory mechanical, electrical or chemical stimuli, has been described in a variety of experimental demyelinating lesions (reviewed by Rasminsky, 1981). Since spontaneous activity has, however, only rarely been detected in rat spinal roots demyelinated with diphtheria toxin, it was concluded previously that demyelination *per se* does not cause hyperexcitability (Bostock, 1982). Other precipitating factors are presumably involved. Our present negative results support that conclusion.

This work was supported by grants to T.A.S. from the Multiple Sclerosis Society of Great Britain, and the Brain Research Trust.

REFERENCES

BOSTOCK, H. (1982). Conduction changes in demyelination. In *Abnormal Nerves and Muscles as Impulse Generators*, ed. CULP, W. & OCHOA, J. New York: Oxford University Press.

BOSTOCK, H. (1983). The strength–duration relationship for excitation of myelinated nerve: computed dependence on membrane parameters. *J. Physiol.* **341**, 59–74.

BOSTOCK, H., FORSTER, I. C., SEARS, T. A. & SHERRATT, R. M. (1981). Simultaneous mapping of thresholds and membrane currents along undissected single nerve fibres. *J. Physiol.* **312**, 8–9*P*.

BOSTOCK, H. & SEARS, T. A. (1978). The internodal axon membrane: electrical excitability and continuous conduction in segmental demyelination. *J. Physiol.* **280**, 273–301.

BOSTOCK, H., SHERRATT, R. M. & SEARS, T. A. (1978). Overcoming conduction failure in demyelinated nerve fibres by prolonging action potentials. *Nature, Lond.* **274**, 385–387,

BRISMAR, T. (1981). Electrical properties of isolated demyelinated rat nerve fibres. *Acta physiol. scand.* **113**, 161–166.

CHIU, S. Y. & RITCHIE, J. M. (1981). Evidence for the presence of potassium channels in the paranodal region of acutely demyelinated mammalian single fibres. *J. Physiol.* **313**, 415–437.

COPPIN, C. M. L. & JACK, J. J. B. (1971). Internodal length and conduction velocity of cat muscle afferent nerve fibres. *J. Physiol.* **222**, 91*P*.

DAVIS, H. (1923). The relationship of the 'chronaxie' of muscle to the size of the stimulating electrode. *J. Physiol.* **57**, 81–82*P*.

FITZHUGH, R. (1962). Computation of impulse initiation and saltatory conduction in a myelinated nerve fiber. *Biophys. J.* **2**, 11–21.

HILL, A. V. (1935). The intensity–duration relation for nerve excitation. *J. Physiol.* **83**, 30–31*P*.

HILL, A. V. (1936). Excitation and accommodation in nerve. *Proc. R. Soc.* B **119**, 305–355.

HUXLEY, A. F. & STAMPFLI, R. (1949). Evidence for saltatory conduction in peripheral myelinated nerve fibres. *J. Physiol.* **108**, 315–339.

LAFONTAINE, S., RASMINSKY, M., SAIDA, T. & SUMNER, A. J. (1982). Conduction block in rat myelinated fibres following acute exposure to anti-galactocerebroside serum. *J. Physiol.* **323**, 287–306.

LAPICQUE, L. (1907). Recherches quantitatifs sur l'excitation électrique des nerfs traité comme un polarisation. *J. Physiol., Paris* **9**, 622–635.

LUSSIER, J. J. & RUSHTON, W. A. H. (1952). The excitability of a single axon in a nerve trunk. *J. Physiol.* **117**, 87–108.

NOBLE, D. & STEIN, R. B. (1966). The threshold conditions for initiation of action potentials by excitable cells. *J. Physiol.* **187**, 129–162.

RASMINSKY, M. (1978). Physiology of conduction in demyelinated axons. In *Physiology and Pathobiology of Axons*, ed. WAXMAN, S. G. New York: Raven Press.

RASMINSKY, M. (1981). Hyperexcitability of pathologically myelinated axons and positive symptoms in multiple sclerosis. In *Advances in Neurology*, vol. 41, ed. WAXMAN, S. G. & RITCHIE, J. M. New York: Raven Press.

RASMINSKY, M. & SEARS, T. A. (1972). Internodal conduction in undissected demyelinated nerve fibres. *J. Physiol.* **227**, 323–350.

SEARS, T. A., BOSTOCK, H. & SHERRATT, R. M. (1978). The pathophysiology of demyelination and its implication for the symptomatic treatment of multiple sclerosis. *Neurology* **28**, 21–26.

TASAKI, I. (1939). The strength duration of the normal, polarised and narcotised nerve fibre. *Am. J. Physiol.* **125**, 367–379.

WEISS, G. (1901). Sur la possibilité de rendre comparables entre eux les appareils servant a l'excitation électrique. *Archs ital. Biol.* **35**, 413–446.